



Fabrication and Characterization of Poly Vinyl Alcohol/ Poly Vinyl Pyrrolidone/MnTiO₃ Nanocomposite Membranes for PEM Fuel Cells

¹Abdol Mohammad Attaran,²Khadijeh Hooshyari,²Mehran Javanbakht,
and ³Morteza Enhessari

¹Department of Chemistry, Payame Noor University, Delijan, I.R. Iran

²Department of Chemistry, Amirkabir University of Technology, Tehran, I.R. Iran

³Department of Chemistry, Islamic Azad University, Naragh Branch, Naragh, I.R. Iran

(Received: August 10, 2012; Accepted in Revised Form: February 12, 2013)

Abstract: PVA (poly vinyl alcohol)-MnTiO₃ (PM) and PVA-PVP (poly vinyl pyrrolidone)-MnTiO₃ (PPM) nanocomposite membranes have been prepared with solutions casting method. Glutaraldehyde (GA) was used as cross linking agent. The results showed that the proton conductivity and water uptake of the nanocomposite membranes due to hydrophilic nature of MnTiO₃ nanoparticles were higher than that of the PVA membrane. PPM membranes containing 5 wt. % of MnTiO₃ nanoparticles and PVA:PVP, 80:20, demonstrated higher thermal stability, water uptake (310%) and proton conductivity (2.1×10^{-2} S/cm) than PM membranes, due to hydrophilic effect of PVP, which can make strong hydrogen-bonding, intense intra-molecular interaction and reduce the crystallinity of the PVA polymer.

Key words: PEM fuel cells · Poly vinyl alcohol · Poly vinyl pyrrolidone · Nanocomposite membranes · Proton conductivity

INTRODUCTION

Polymer Electrolyte Membrane Fuel cells (PEM Fuel cells) display the highest power densities compared to the other type of fuel cell [1]. Polyperfluorosulfonic acid (PFSA) membranes, such as Nafion, are the most common type of polymeric membranes used for PEMFC due to their excellent chemical, mechanical, thermal stability and high proton conductivity in their hydrated state [2]. But, one great drawback of Nafion membranes is their dehydration at temperatures above 80°C, causing a dramatic decrease in their proton conductivity and mechanical stability [3]. Poly vinyl alcohol (PVA) is a cheap polymer having excellent film forming and adhesive properties, good chemical and mechanical stability and high potential for chemical cross-linking. However, PVA has highly swelling and low proton conductivity [4]. According to research done, the addition of hygroscopic metal oxide nanoparticles such as SiO₂ and TiO₂ to the PVA polymer matrix [5], crosslinking of PVA with aldehyde and dialdehydes and blending PVA with other polymer such as Nafion, SPEEK improve its water uptake and proton conductivity [6].

Experimental

Material: The Poly vinyl alcohol (99% hydrolyzed, average Mw=145,000, Merck, Germany), glutaraldehyde (25 wt. % solution in water, Merck) and Poly vinyl pyrrolidone (average Mw=40,000, Sigma, USA) were used as the backbone polymer, cross-linking agent and blend polymer with PVA membrane respectively. MnTiO₃ nanoparticles with a particle size range of 22-30 nm were synthesized by Dr Enhessari *et al.* [7] and used as modifier.

Preparation of Membranes: PVA membrane, PVA/MnTiO₃ and PVA/PVP/MnTiO₃ nanocomposite membranes were synthesized with solution casting method. The nanocomposite membranes were named PM and PPM respectively. Membranes were synthesized by dissolving PVA and MnTiO₃ nanoparticle in DI water under stirring at 80 °C. Water solutions of PVP were separately prepared and mixed with PVA solutions (PVA/PVP 80:20). Then GA was slowly added. The well-mixed homogeneous and viscous solution was transferred to petri-glass dishes. Then the membranes were dislodged from the petri-glass dishes easily and then stored in DI water until experiments were performed.

Corresponding Author: Mehran Javanbakht, Department of Chemistry, Amirkabir University of Technology, Tehran, I.R. Iran. E-mail: mehranjavanbakht@gmail.com.

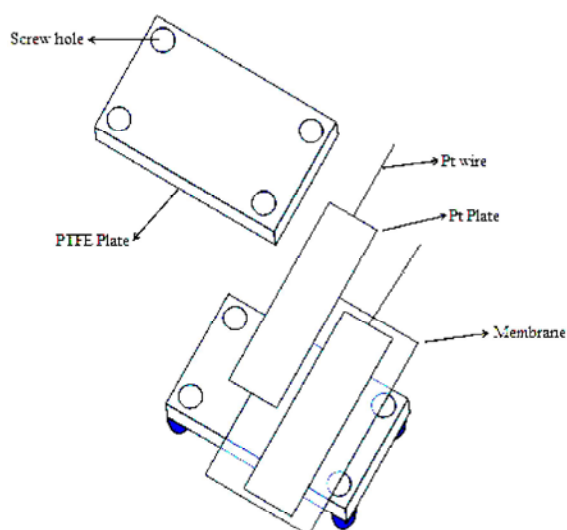


Fig 1: Schematic diagram of cell for measurement of membrane proton conductivity.

Water Uptake Measurement: Water uptake measurements for all membranes were conducted by immersing the membrane samples into deionized water at room temperature for 24 h to guarantee equilibrium. Subsequently, the samples were taken out and removed the residual water on surfaces and weighed immediately. The samples were then dried in vacuum at 80 °C for 24 h and weighed again. The water uptake (SW) was calculated by the following equation:

$$SW = \frac{W_{wet} - W_{dry}}{W_{dry}} \times 100$$

Where, W_{wet} and W_{dry} are weights of wet and dry membrane, respectively.

Proton Conductivity Measurement: The proton conductivity of membrane was obtained by three-electrode method using AC impedance spectroscopy with PGSTAT303N potentiostat/Galvanostat (Ecochemie). Fully hydrated samples of size 1 × 1 cm were sandwiched between two platinum plates electrodes of the same size. Fig. 1 shows a measurement cell for measuring proton conductivity of membranes. The spectra were recorded with signal amplitude of 20 mV in the frequency range of 100Hz–1MHz with 100 points. The resistance of the membranes were determined from the high-frequency intercept of the impedance. The conductivity of the membranes were calculated using the equation ($\sigma = L/RA$), Where, σ , L, R and S, respectively, refer to proton

conductivity ($S\ cm^{-1}$), thickness (cm), resistance from the impedance data (Ω) and cross-sectional area (cm^2), of the membranes.

ATR-FTIR and SEM Measurements: The ATR-FTIR spectra ($600\text{--}4000\ cm^{-1}$, resolution $4\ cm^{-1}$) were recorded with a Bruker Equinox 55 using an attenuated total reflectance (ATR, single reflection) accessory purged with ultra dry compressed air. SEM study of the samples were performed on a Jeol JSM-5600 SEM. This instrument was equipped with an EDX (x-ray microanalysis) system with a sufficient sensitivity to detect elements with low atomic numbers. To obtain cross sectional images of the samples they were freeze-fractured in liquid N_2 and coated with a thin layer of gold ($\sim 10\ nm$), using an automated sputter coater to improve the resolution and quality of the SEM images.

Thermal Stability Measurement: To investigate the thermal stability of the samples, thermogravimetric analysis (TGA) of the membranes were carried out using a 2050 TGA (TA Instruments) system in nitrogen atmosphere. The programmed heating rate was $20\ ^\circ C/min$. The differential scanning calorimetry (DSC) measurements were performed on the dried samples, in the range of temperature between 25 and $600\ ^\circ C$ using a Mettler DSC 823. The scanning rate was $10\ ^\circ C/min$ in nitrogen flow.

RESULTS AND DISCUSSION

Water Uptake and Proton Conductivity Measurements: PM and PPM nanocomposite membranes with 5 wt. % of $MnTiO_3$ nanoparticle showed higher water uptake, 270% and 310%, respectively and proton conductivity, 5.4×10^{-3} and $2.1 \times 10^{-2}\ S\ cm^{-1}$, respectively, compared with PVA, 230% and $9 \times 10^{-4}\ S\ cm^{-1}$, based membrane. The improved water uptake was attributed to the hydrophilic nature of the $MnTiO_3$ nanoparticles and the increased surface areas of these nanoparticles compared with TiO_2 nanoparticles, which can increase the proton conductivity.

The results obtained from the Nyquist plots (Fig. 2a) displayed that PPM nanocomposite membranes containing 5 wt. % of nanoparticles and (PVA:PVP 80:20) displayed a lower resistance (higher proton conductivity) than that of PVA and PM membranes. The addition of PVP, which can reduce the crystallinity of the PVA polymer, result in an increase the amorphous phases of PVA polymer matrix and enhanced membranes swelling [8]. Bod plot (Fig. 2b) confirms the result obtained from Nyquist plot.

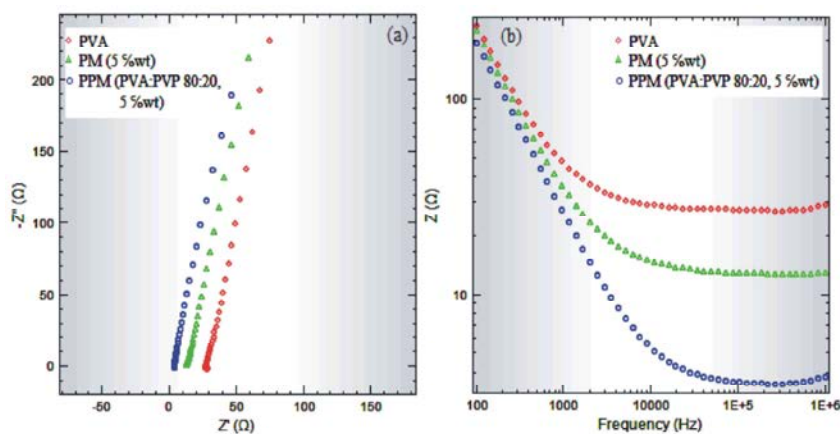


Fig 2: Nyquist (a) and Bode modulus (b) plots of PVA and nanocomposite membranes.

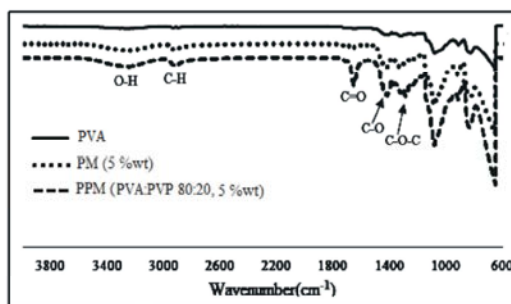


Fig 3: FT-IR ATR spectra of PVA and nanocomposite membranes.

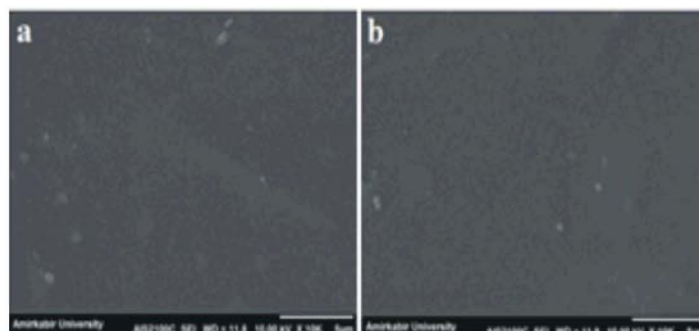


Fig 4: SEM images of the (a) PM and (b) PPM (PVA: PVP 80:20) nanocomposite membranes with 5 wt. % of MnTiO₃ nanoparticles.

FT-IR ATR Spectra: Fig. 3 shows the typical FT-IR ATR spectra measured for PVA, PM and PPM membranes. The broad bands at around 3258 cm⁻¹ and 3274 cm⁻¹ are observed due to -OH groups in the PVA chain [9]. The low intensity of the -OH peak, due to better cross-linking of PVA with GA, was also clearly observed [10].

The presence of -OH groups in the PVA chain allows the reaction with -CHO groups in GA and formation of ether bonds (C-O-C) PVA due to has a dense structure. The bands at 1250-1270 cm⁻¹ were attributed to

the ether bonds (C-O-C) [1]. The peaks at 1650-1655 cm⁻¹ suggests the presence of such free C=O groups [10]. Increase in the intensity of the C=O peak in PPM membranes (PVA: PVP 80:20, 5 wt.%) compared PM (5 wt.%) membranes, confirmed a present of C=O groups of PVP in addition of C=O groups of GA.

C-N group of PVP due to the overlapping by -C=O group, could not visibility. The peaks at 1419-1421 cm⁻¹ were assigned to the C-O groups of PVA based membranes. The band at 2907 cm⁻¹ was attributed to the C-H groups [11].

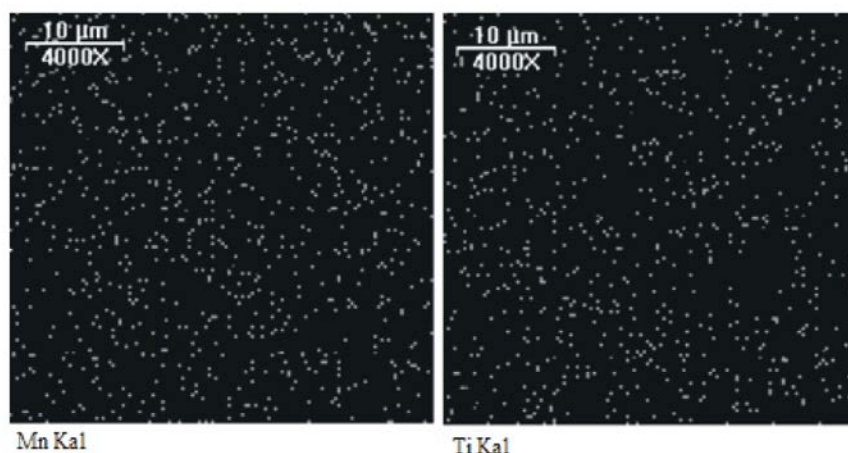


Fig 5: EDX distribution of Mn and Ti nanoparticles in the PPM (PVA: PVP 80:20, 5 wt. %) nanocomposite membrane.

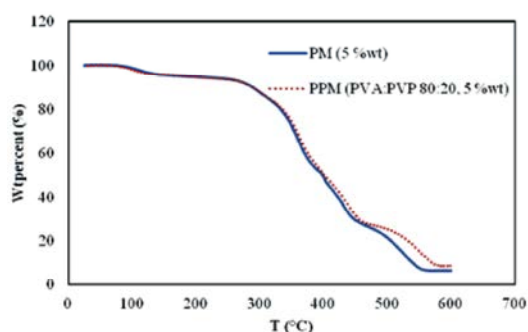


Fig 6: TGA plots of PM and PPM nanocomposite membranes.

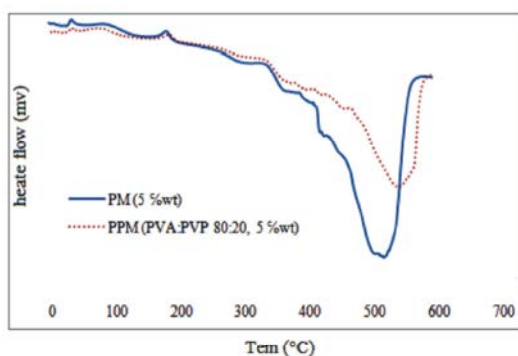


Fig 7: DSC plots of PM and PPM nanocomposite membranes.

SEM-EDX Images: From the SEM images shown in Fig. 4, the MnTiO₃ nanoparticles in the PM (Fig. 4a) and PPM (Fig. 4b) nanocomposite (PVA: PVP 80:20) with 5 wt. % of nanoparticles, can be clearly seen. Dispersion of the Mn and Ti nanoparticles in the cross-section of PPM nanocomposite membrane, with 5 wt. % of MnTiO₃

nanoparticles and PVA: PVP 80: 20, was investigated by the EDX mapping images and displayed in Fig.5. EDX distribution demonstrated homogenous distribution of Mn and Ti nanoparticles in the PPM membranes.

DSC analysis and respectively displayed in Figs. 6 and 7. Nanocomposites demonstrated a higher thermal stability than PVA based membrane. Incorporation of MnTiO₃ nanoparticles in the PVA polymer matrix would fill these free volumes and would cause need to more energy for starting segmental motion. PPM nanocomposite membranes due to hydrogen-bonding of PVP with PVA and intense intra-molecular interaction, displayed a higher Tm and thermal stability than PM membranes. Fig. 7 shows that, Tm of PM and PPM nanocomposite membranes was transferred to above 500°C and it's very higher than of Tm of PVA (230°C).

Thermal Analysis: The thermal stability of the PM and PPM (PVA: PVP, 80:20) nanocomposite membranes with 5 wt.% of MnTiO₃ nanoparticles were evaluated with TGA and thus the result obtained from TGA and DSC analysis shows the improved potentials of the PPM (PVA: PVP, 80:20) nanocomposite membranes for higher temperature operation of fuel cells applications.

CONCLUSION

PVA-PVP-MnTiO₃ nanocomposite membranes were synthesized by solutions casting method and characterized for PEM fuel cells with high proton conductivity. The nanocomposite membranes with 5 wt. % of nanoparticles, due to hydrophilic nature of MnTiO₃ nanoparticles and PVP, displayed higher water uptake and proton conductivity than PVA based membranes. High

hydrophilic properties of PVP play an important role in reducing of PVA crystallinity and increase its water uptake and proton conductivity. PPM (PVA:PVP 80:20, 5 wt.%) nanocomposite membranes due to strong interactions of PVP with PVA and intra-molecular contacts displayed a higher thermal stability than PM (5 wt.%) membranes. FT-IR ATR spectra confirmed characteristic peaks of -OH, C-O-C, C=O, C-H and C-O groups at nanocomposite membranes.

REFERENCES

1. Schoots, K., G.J. Kramer and B.C.C. Vander Zwaan, 2010. "Technology learning for fuel cells: An assessment of past and potential cost reductions", *Energy Policy*, 38: 2887-2897.
2. Nikhil, H., K. Dunn and R. Datta, 2005. "Synthesis and characterization of Nafion-MO₂ (M = Zr, Si, Ti) nanocomposite membranes for higher temperature PEM fuel cells", *Electrochimica Acta*, 51: 553-560.
3. Chen, C.Y., J.I. Garnica, M.C. Duke, R.F. Dalla, A.L. Dicks and J.C. Diniz, 2007. "Nafion/polyaniline/silica composite membranes for direct methanol fuel cell application", *Power Sources*, 166: 324-330.
4. Yang, C.C., W.C. Chien and Y.J. Li, 2010. "Direct methanol fuel cell based on poly (vinyl alcohol)/titanium oxide nanotubes/poly (styrene sulfonic acid) (PVA/nt-TiO₂/PSSA) composite polymer membrane", *Journal of Power Sources*, 195: 3407-3415.
5. Kim, D.S., H.B. Park, J.W. Rhim and Y.M. Lee, 2004. "Preparation and characterization of crosslinked PVA/SiO₂ hybrid membranes containing sulfonic acid groups for direct methanol fuel cell applications", *Journal of Membrane Science*, 240: 37.
6. Qiao, J., T. Hamaya and T. Okada, 2005. "New highly proton-conducting membrane poly (vinyl pyrrolidone) (PVP) modified poly (vinyl alcohol) / 2-acrylamido-2-methyl-1-propanesulfonic acid (PVA-PAMPS) for low temperature direct methanol fuel cells (DMFCs)", *Polymer*, 46, 10809-10816, (2005).
7. Enhessari, M., A. Parviz, E. Karamali and K. Ozaee, 2012. "Synthesis, characterisation and optical properties of MnTiO₃ nanopowders", *Experimental. Nanoscience*, 7: 327-335.
8. Beydaghi, H., M. Javanbakht, H. Salar Amoli, A. Badii, Y. Khaniani, M. Ganjali, P. Norouzi and M. Abdouss, 2011. "Synthesis and characterization of new proton conducting hybrid membranes for PEM fuel cells based on poly(vinyl alcohol) and nanoporous silica containing phenyl sulfonic acid", *Journal of Hydrogen Energy*, 36: 13310-13316.
9. Mansur, H.S., C.M. Sadahira, A.N. Souza and A.A.P. Mansur, 2008. "FTIR spectroscopy characterization of, poly (vinyl alcohol) hydrogel with different hydrolysis degree and chemically crosslinked with glutaraldehyde", *Journal of Material Science Engineering*, 285: 39-48.
10. Kang, M.S., Y.J. Choi and S.H. Moon, 2002. "Water-swollen cation-exchange membranes prepared using poly (vinyl alcohol) (PVA)/poly (styrene sulfonic acid-co-maleic acid) (PSSA-MA)", *Journal of Membrane Science*, 207: 157-70.
11. Suzuki, M., S. Ito and T. Kuwahara, 1983. "Preparation of red organic pigment with phenylated silica gel as core", *Journal of Bull Chem Soc. Jpn*, 56: 956-7.